- 1 TITLE: High Resolution, High Aspect Ratio Printed
- and Plated Metal Conductors Utilizing Roll-to-Roll
- Micro-Scale UV Imprinting with Prototype
  - Imprinting Stamps
- 5 AUTHOR NAMES
- 6 Krystopher S. Jochem, Wieslaw J. Suszynski, C. Daniel Frisbie\*, Lorraine F. Francis\*
- 7 AUTHOR ADDRESS
- 8 Department of Chemical Engineering and Materials Science, University of Minnesota,
- 9 421 Washington Avenue S.E., Minneapolis, Minnesota 55455, United States
- 10 KEYWORDS
- 11 Roll-to-Roll UV Imprinting, High-Resolution Printed Conductors, High-Aspect Ratio Roll-to-
- Roll Micro Molding, Low Cost Roll-to-Roll Imprinting Stamp Fabrication, Printed Electronics

### **ABSTRACT**

Micron-scale, high aspect ratio features were imprinted by a roll-to-roll process into a UV-curable polymer and used to create high current carrying conductive networks on plastic substrates. A stamp fabrication method was developed to create low-cost, rapidly-produced roll-to-roll imprinting stamps, which can mold features from 3 μm to 1 mm wide. Isolated raised features 50 μm high were molded from a 25 μm thick layer of UV-curable resin by displacing resin into raised features in the stamp. Substrates with imprinted capillary channels were used to form electrical conductors by printing a silver ink into reservoirs connected to the channels and allowing capillary flow to coat the channel. Copper electroless plating then filled the channels. The conductors demonstrate high resolution, high aspect ratio (~5:1, height: width), low resistance per length, and easy integration into networks. This roll-to-roll imprinting process provides a foundation for high-throughput manufacturing of high resolution printed electronics.

### **TEXT**

### **Introduction:**

Printing processes using high-throughput, roll-to-roll techniques have promise for manufacturing of low-cost electronic circuits on flexible substrates. Printed electronics have a wide range of applications including radio frequency identification devices<sup>12</sup>, displays<sup>1,4</sup>, photovoltaics<sup>5,6</sup>, sensors<sup>2,9</sup>, and integrated circuits<sup>10,11</sup>. Additive manufacturing techniques, such as printing, are beneficial for device fabrication, because there is very little wasted material, unlike traditional etching-based, subtractive fabrication techniques<sup>12,13</sup>.

A range of printing techniques have been used to create printed electronics including gravure printing, inkjet printing, and aerosol jet printing among others<sup>1-21</sup>. However, these printing techniques face two critical challenges. First, the small feature sizes (e.g., < 10 µm)<sup>22</sup> that are necessary for increasing device density and transistor switching speed<sup>20,24</sup> are difficult to realize. Second, these techniques, implemented roll-to-roll, lack precision in aligning the multiple layers of printed ink that are necessary in devices such as thin film transistors<sup>26</sup>. Current roll-to-roll techniques lack alignment precision due to difficulty in achieving precise positional correlation between the print head or roll and the substrate as well as deformation of the flexible plastic substrates (webs) from applied tension by the web handling equipment<sup>26</sup>.

The Self-aligned Capillarity-Assisted Lithography for Electronics process (SCALE)<sup>27-30</sup> was developed to overcome these challenges. The process is outlined in Figure 1. In the SCALE process, a high-resolution master pattern is made by photolithography and the pattern is then used to make stamps. The stamps are then employed in a micro-scale UV-imprinting to mold networks of capillary channels and device structures onto a flexible plastic substrate. Next, inkjet printing is used to deposit electrically functional inks into reservoirs connected to capillary channels and devices. Capillarity then drives ink flow along the channels. Hence, the printing resolution demands are dictated by the reservoir size and not the size of capillaries and devices, which are much smaller. Since the imprinted substrate is formed in a single processing step from a master pattern with precise features designed to control ink flow and placement, layers of ink can be aligned in multilayer devices such as transistors<sup>22,27</sup> and supercapacitors<sup>26</sup>. Conductive networks with high current carrying capability are needed to connect the devices for optimal circuit performance.

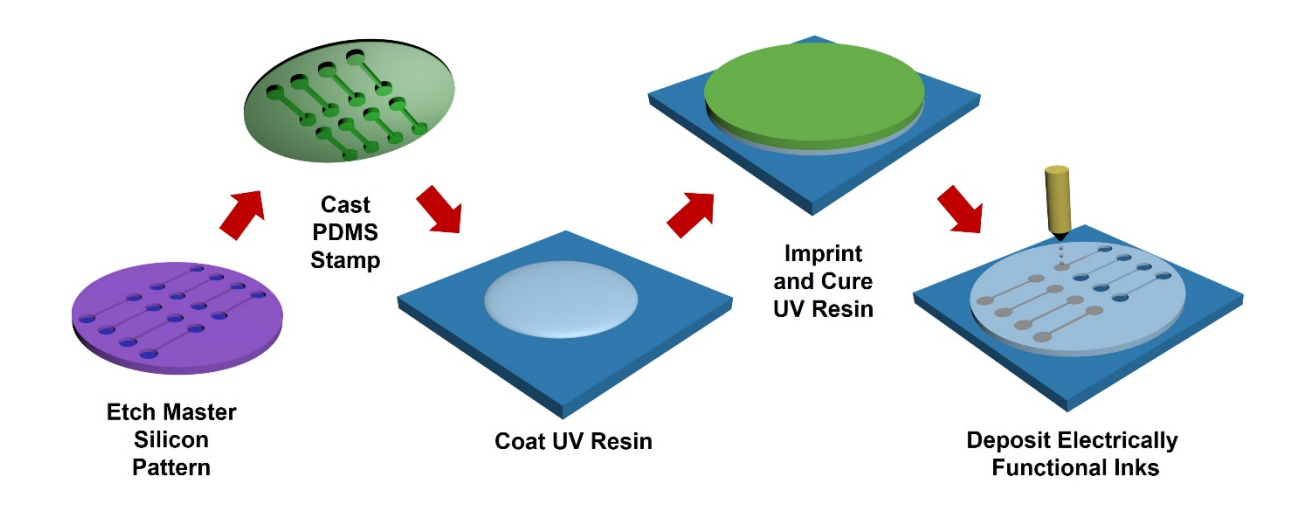


**Figure 1.** Schematic overview of the SCALE process for forming high resolution, high aspect ratio electronic devices on a plastic substrate.

Improving current carrying capability while maintaining narrow conductor line widths requires the design of low resistance, high aspect ratio conductors, where aspect ratio ( $\varepsilon$ ) is defined as the height (H) of the conductive line divided by its width (W). Considering conductive lines with rectangular cross-sections, conductor resistance per length (R/L) is related by aspect ratio and width:

10 
$$R/L = \rho/A = \rho/(\varepsilon W^2) \tag{1}$$

where  $\rho$  is the resistivity of the conductor and A is the cross-sectional area perpendicular to the direction of current flow ( $A = H \cdot W$ ). Traditional printing processes such as inkjet and gravure printing typically produce conductive lines with aspect ratios in the range of 0.01 to 0.05. 12.06.22.25.31 With the SCALE process, we have previously demonstrated metal conductors 4.1  $\mu$ m wide and 2.5  $\mu$ m thick, which gives an aspect ratio of 0.6.24 While this result is promising, further development is needed to achieve higher aspect ratios, longer conductor lengths, and improved performance.25 Deeper capillary channels would allow both higher  $\varepsilon$  and lower R/L in SCALE conductors. Deeper channels are also expected to promote increased travel distance of inks

contained in the channels<sup>32,33</sup>. To produce conductors with this desirable geometry, roll-to-roll imprinting stamps capable of achieving micron scale resolution and high  $\varepsilon$  are needed.

Past work on roll-to-roll imprinting has demonstrated that the process is capable of forming feature sizes of 100's of nm on flexible plastic films<sup>12-18</sup>, but little attention has been given to aspect ratio. Some of this past work has focused on the roll-to-roll implementation of nanoimprint lithography<sup>30</sup>, a method that involves pressing a nanostructured stamp through a UV-curable liquid layer such that the stamp displaces the liquid completely, to open windows to the material below for subsequent etching or deposition. Another emphasis in past work is the formation of repetitive structures in the surface of the coating for applications including the formation of moth-eye lens arrays<sup>30</sup>, and waveguides<sup>30,41</sup>. However, to our knowledge, there have been no reports to-date on roll-to-roll UV imprinting of the feature types needed for SCALE conductors (*i.e.*, 10's of micron tall, discrete features with high aspect ratio from polymer-based imprinting stamps).

In this work, we report on the use of roll-to-roll imprinting and the SCALE process to create high aspect ratio conductors. A key advance is the development of roll-to-roll UV imprinting process with custom made, rapidly produced and easily exchanged prototype imprinting stamps. Most methods for fabricating stamps for UV roll-to-roll imprinting require complex or high cost processing, or are not capable of molding structures that are much higher than they are wide (high aspect ratio)<sup>22,25,8</sup>. In the process described here, stamps are fabricated from a silicon wafer master pattern using liquid casting of low-cost silicone. A series of stamps is then bound to a polyethylene terephthalate (PET) film to form a stamp assembly. The PET acts as a low-cost, high strength backing material for attachment to the roll-imprinting drum. Single or multiple pattern designs can be produced in a short period of time for testing purposes or for single imprinting runs. A second key advance is the formation of high aspect ratio, low resistance

- 1 conductive networks on flexible substrates. These conductors facilitate the low-resistance
- 2 electrical connection between multiple locations (up to nine demonstrated here), while only
- 3 requiring ink deposition in a single location.

5

6

7

8

9

10

11

12

13

14

15

16

17

18

19

20

21

22

23

# **Experimental Section:**

#### Master Pattern Fabrication

Traditional photolithography techniques were used to prepare silicon wafer master patterns for fabricating roll-to-roll imprinting stamps, as shown in Figure S1 in the supporting information. Two basic designs were employed: recessed features and raised features (Fig. S2). For patterns designed to create a recessed feature design, a 10.2 cm diameter silicon wafer was dehydrationbaked on a hot plate at 120 °C for 5 min. The wafer was then exposed to a hexamethyldisilazane environment for 5 min. Shipley 1813 positive tone photoresist was spin coated on the wafer at 3000 rpm for 30 s followed by a soft-bake on a hot plate at 115 °C for 1 min. The photoresist was then exposed through a photomask using a Karl Suss MA6 contact mask aligner in Hard Contact mode for 6 s. The wafer was then baked at 115 °C for 1 min. The exposed wafer was developed in Microposit 351 Developer mixed with water (1:5) for 30 s followed by a rinse in de-ionized water for 3 min. The resist was then hard baked at 120 °C for 1 min. Etching was performed in a Plasma Therm SLR-770 Deep Reactive Ion Etcher using the BOSCH process at an etch rate of approximately 3 µm/min to achieve desired feature depth. After etching, the photoresist was stripped from the wafer using acetone, methanol, isopropanol and de-ionized water in series. The etched wafer was then exposed to trichloro(1H,1H,2H,2H-perfluorooctyl)silane vapor (Sigma Aldrich) overnight in a reduced pressure chamber to form an anti-stick monolayer over the surface of the wafer.

A similar process was used to produce master patterns for the raised feature design. A 10.2 cm diameter silicon wafer was dehydration-baked on a hot plate at 200 °C for 5 min. Futurrex NR71-3000P negative tone photoresist was spin coated onto the wafer at 1500 rpm for 45 s followed by a soft-bake on a hot plate at 150 °C for 1 min. The photoresist was then exposed through a photomask using a Karl Suss MA6 contact mask aligner in Hard Contact mode for 20 s. Then the wafer was baked at 100 °C for 1 min. The exposed wafer was developed in Futurrex RD6 for 3 min followed by rinsing in de-ionized water for 3 min. Etching was performed in a Plasma Therm SLR-770 Deep Reactive Ion Etcher using the BOSCH process at an etch rate of approximately 1.2 µm/min (slower since all of the wafer surface except the raised features is etched). After etching, the photoresist was stripped from the wafer using Futurrex RR41 followed by rinsing in de-ionized water and the formation of an anti-stick fluorinated monolayer as described above.

# Stamp Assembly Fabrication

Imprinting stamps were formed from master patterns by casting liquid silicone resin, as described in Figure 2. The master pattern wafer was secured in the base of a Petri dish. About 35 g of polydimethylsiloxane (PDMS) (Sylgard 184, Dow Corning) was prepared by mixing with a monomer to curing agent ratio of 10:1 by weight and degassing in a vacuum chamber until all air bubbles were removed based on visual observation of the PDMS transitioning from opaque to clear. Then, the PDMS was poured over the wafer and cured for 2 hr at 75 °C (Fig. 2a). The solidified PDMS was then removed and annealed, first at 120 °C for 2 hr and then at 220 °C for 2 hr to achieve its final hardness of 57 Shore A (Fig. 2b). The PDMS stamps were then trimmed to an octagon shape for ease of installation on the roll imprinting stamp assembly (Fig. 2c). A piece of 36 µm thick silicone coated release film (Drytac – Hotpress CRP 41082) was used as a backing

material for the stamp assembly. Sylgard 184 PDMS mixed with a monomer to curing agent ratio
of 10:4 was used as an adhesive to bind the cast PDMS to the silicone coated PET, and this was
cured at 45 °C for 24 hrs (Figs. 2d and 2e). Mounting holes were punched in the stamp assembly
to accommodate a clamp, which secures the stamp assembly to the imprinting drum (Fig. 2f).
Then, the finished stamp assembly was wrapped around the imprinting drum and clamped in place.
The seam in the stamp assembly was covered with tape (3M, 1280) and silicone release spray

(Dow 316) to prevent accumulation of UV-curable resin in the seam during imprinting (Fig. 2g).

7

8

9

10

(a) (d) (e) (f) (g)

**Figure 2.** Schematic of the stamp fabrication process for high-aspect ratio, micron scale imprinting stamps: (a) PDMS casting and curing on a silicon wafer master pattern, (b) thermal annealing of

the cured PDMS to increase hardness, (c) trimming of the PDMS to facilitate assembly of a full roll stamp, (d) application of PDMS adhesive onto silicone coated PET, (e) attaching the PDMS castings to the silicone coated PET to fabricate a roll imprinting stamp, (f) trimming excess PDMS and cutting mounting holes in the PDMS stamp for clamping to the imprinting drum, and (g) wrapping of the finished stamp around the imprinting drum.

5 6

7

8

9

10

11

12

13

14

15

16

17

18

19

20

21

22

23

24

25

26

1

2

3

4

# Roll-to-Roll Imprinting

Roll-to-roll imprinting was performed on a commercial roll-to-roll imprinting machine from Carpe Diem Technologies, as shown in Figure 3. A clear 127 µm thick and 12.1 cm wide PET web (DuPont – Teijin Melinex ST505 slit to width by Tekra) was used as the base substrate. In a typical process, the web is cleaned by a rubber roller to remove any dust and then passed to the coating station. A micro-gravure roll rotating in the opposite direction to the web movement and at the same speed as the web (reverse micro-gravure coating) is used to deposit a thin layer of a liquid UV-curable resin (NOA-73, Norland Products) onto the PET web. The micro-gravure roller, manufactured by Harper Corporation of America, has cavities designed to produce a 25 µm thick coating. The gravure cells are approximately hexagonal in shape with a width of  $\sim$ 225 µm, a depth of ~35 µm, and a volume of ~1500 pL. An optical image and a confocal height profile are provided in Figure S3. The viscosity of the resin (130 mPa•s)<sup>44</sup> is low enough for the resin to flow into features during imprinting, but still high enough to control the spread or flow of the coated layer on the web between the coating and imprinting stations. The coating thickness used in this work was approximately 25 µm. The reverse micro-gravure coating process is shown in detail in Figure S4. The coated web then passes to the imprinting station where the web is pressed into the imprinting stamp by both the 8.9 N web tension and an air knife, which directed a pressurized air flow locally to the back side of the web at the point of contact between the coated substrate and the stamp. While the UV-curable resin is in contact with the imprinting stamp, the resin is cured by a high intensity mercury arc lamp UV light source (~0.57 W/cm<sup>2</sup> average), as shown in Figure

- 1 S5. The length of web illuminated as it passes around the imprinting drum is only 1.5 cm, so a
- 2 web speed of 10.2 cm/min is used to provide a total dosage of 4.7 J/cm to the web, which is
- 3 sufficient to achieve full solidification of the UV resin. The imprinted web was then rewound on
- 4 the collection drum.

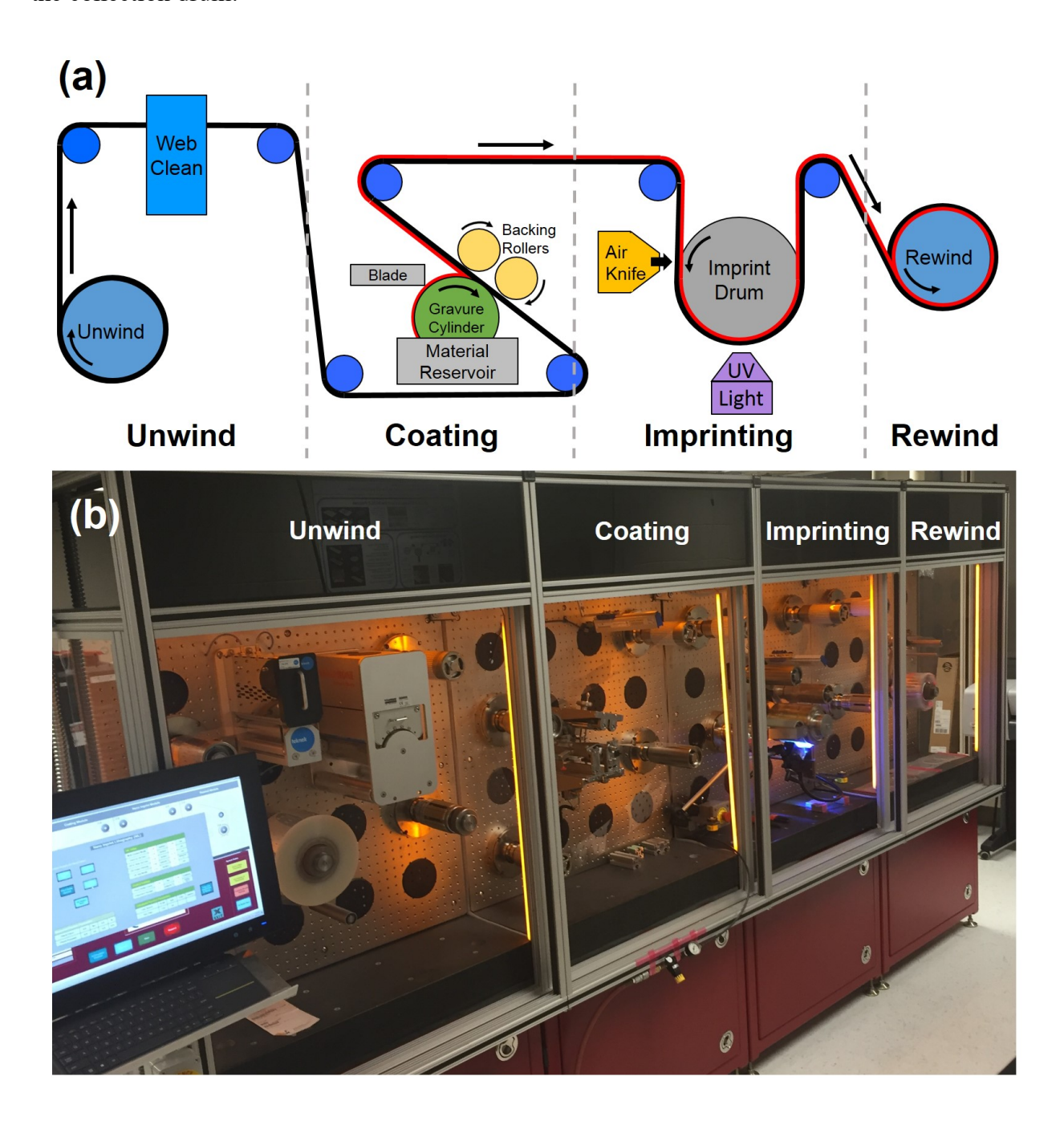


**Figure 3.** (a) Schematic diagram of the roll-to-roll imprinting process used in this work consisting of Unwind, Coating, Imprinting, and Rewind sections, and (b) photograph of the roll-to-roll imprinting apparatus to show scale and overall layout.

3

5

6

7

8

9

10

11

12

13

14

15

16

17

18

19

20

21

22

23

24

25

1

2

# **Conductor Fabrication**

Conductors were formed on the imprinted substrates by inkjet printing followed by electroless plating, as shown in Figure S6. A drop-on-demand inkjet printer (Microfab) with an 80 µm nozzle was used to deposit a controlled volume of an aqueous, particle free silver ink (Electroninks, Grade El) to fill the reservoirs. After allowing ~ 1 min for capillary flow, the printed substrate was placed on a hotplate at 100 °C for 5 min. This process was repeated for a second layer of ink to improve silver uniformity. Then, an electroless copper plating solution was prepared from 2.7 g CuSO<sub>4</sub>·5H<sub>2</sub>O (Alfa Aesar), 10.2 g ethylenediaminetetraacetic acid disodium salt (Fisher), and 70 ml de-ionized H<sub>2</sub>O in one jar and 3.2 g NaOH (Fisher) and 30 ml de-ionized H<sub>2</sub>O in a second jar. Each jar was sonicated for 60 min to promote the dissolution of the solids. Then, the two solutions were combined with constant stirring and 2 ml formaldehyde (37% solution in water, VWR) was added. The substrates were suspended vertically in the plating bath, which was mixed continually and maintained at room temperature during the copper deposition process. A small quantity of formaldehyde solution (0.4 ml) was added every 30 min during the one hour (recessed capillaries) or four hour (raised capillaries) plating process. The substrates were rinsed with de-ionized water and dried after they were removed from the plating bath.

### Characterization

Optical imaging of the samples was performed on digital microscopes (Keyence VHX and Hyrox KH-7700). Sample cross sections were prepared using a Leica UC6 microtome. SEM imaging of the samples was performed on a JEOL 6610LV SEM and a Hitachi S4700 FESEM. Stamp hardness was measured with a PTC Instruments Model 408 Shore A handheld indenter.

- 1 Stamp tensile storage and tensile loss moduli were measured with a Perkin Elmer DMA 8000
- 2 dynamic mechanical analyzer. Coating thicknesses were measured by a Schut digital micrometer.
- 3 Confocal imaging was performed on a Hyphenated Systems HS200A optical profiler. Feature
- 4 heights were measured using a KLA Tencor P-16 profilometer. Ink contact angle was measured
- 5 with a Kruss DSA 30 drop shape analyzer. Electrical measurements were performed using a
- 6 Keithley 2400 source meter.

# **Results and Discussion:**

### Stamp Fabrication and Properties

The stamp fabrication process is outlined in Figure 2. This process involves relatively low-cost materials and low-complexity processes. To easily exchange stamp patterns and rapidly fabricate new designs, the stamps are fabricated separately and attached to a backing film, which is then secured to the imprinting drum by a clamp system. Fabrication of individual PDMS stamps (Figs. 2a-2c) required attention to curing conditions, as described below. The cured PDMS stamps are secured to a piece of silicone-coated PET to form a stamp assembly (Figs. 2d and 2e). The silicone coating provides a non-stick surface for any UV-curable resin that flows off the stamp face during imprinting to prevent resin accumulation on the stamp assembly. The PET film improves feature dimensional integrity since its high elastic modulus prevents the PDMS from deforming as it is wrapped around the imprinting drum (Figs. 2f and 2g). To adhere the stamps to the backing film, a thin layer of Sylgard 184 PDMS prepared with an increased ratio of curing agent to monomer is used. The increased concentration of curing agent was found to improve the adherence. Five different 10 cm diameter patterns can be included on each roll-to-roll imprinting

stamp assembly. This allows the direct comparison of different pattern designs or pattern depths simultaneously during each imprinting run.

1

2

3

4

5

6

7

8

9

10

11

12

13

14

15

16

17

18

19

20

21

22

23

To produce high current carrying and high-resolution conductive lines by SCALE, the imprinting stamps must be capable of forming features as small as a few microns wide with high aspect ratio,  $\varepsilon$ . These high aspect ratio features make the raised stamp features susceptible to buckling during imprinting, which has a negative effect on pattern reproduction. To improve performance, the effects of stamp curing condition were explored.

Figure 4 shows the effect of stamp curing condition and properties on the imprint quality for a 3  $\mu$ m wide, 20  $\mu$ m deep recessed capillary. Figure 4a shows the imprint result from a stamp prepared using Sylgard's recommended curing conditions, which produce a stamp with Shore A hardness of 46, a tensile storage modulus of 2.6 MPa, a tensile loss modulus of 0.2 MPa, and a tan  $\delta$  of approximately 0.08 at 25 °C and an oscillatory frequency of 1 Hz. Since tan  $\delta$  is significantly less than one, the PDMS stamp is primarily an elastic material. Just to the right of the reservoir, the channel has a wavy pattern, indicating that the narrow, tall protrusion on the stamp has started to bend over during imprinting. Further to the right, the width of the imprinted capillary is  $\sim 20$  $\mu$ m wide where it should be 3  $\mu$ m and ~ 3  $\mu$ m deep where it should be 20  $\mu$ m. This discrepancy indicates that the raised piece of the stamp has completely folded sideways during imprinting. This is further confirmed by the presence of ridges (an artifact of the BOSCH etching process used for the master pattern) running along the base of the capillary which should only be observed on the side walls. Also, Figure 4a shows defects around the circular reservoir where the UV-resin has been excessively extruded from the raised features (see the color gradient in the orange region) due to stamp deformation. Thus, it is necessary to increase the hardness of the imprinting stamp. It has been shown that increasing the curing temperature used to harden Sylgard 184 can increase

its hardness<sup>47</sup>. By performing a three-step curing process including a high temperature annealing at 220 °C, the stamp hardness, tensile storage modulus, and tensile loss modulus, increase to 57 Shore A, 5.1 MPa, and 0.5 MPa, respectively. The increased tensile storage modulus reduces stamp deformation during imprinting and improves feature reproduction. Tan  $\delta$  is approximately 0.1, which still indicates a primarily elastic material. Figure 4b shows the outcome of this modified curing protocol; a much narrower channel ( $\sim 3 \mu m$ ), which is similar to the stamp dimensions, has been formed. All of the flat areas of the imprinted substrate are very level, and there has been no noticeable effects that could be attributed to stamp deformation.

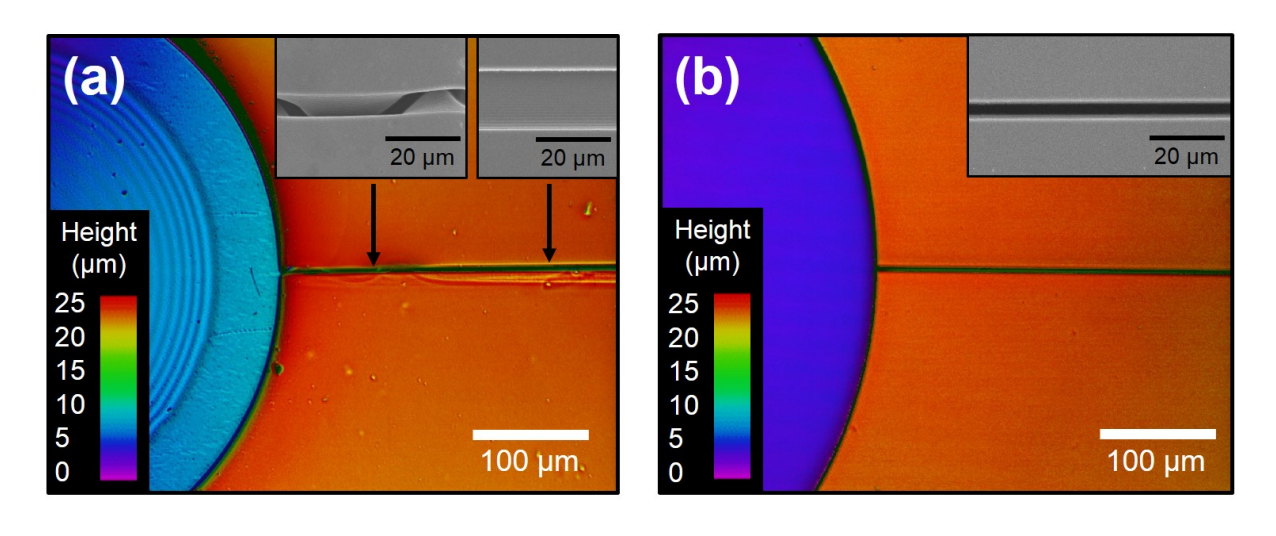


**Figure 4.** Confocal and SEM images of imprinted substrates with recessed features created with stamps of different hardness: (a) PDMS with a Shore A hardness of 46 (tensile storage modulus of 2.6 MPa and tensile loss modulus of 0.2 MPa) and (b) PDMS with a Shore A hardness of 57 (tensile storage modulus of 5.1 MPa and tensile loss modulus of 0.5 MPa). Defects including the rings present in the reservoir and the deformation of the high aspect ratio parts of the stamp (shown by the defects along the narrow, recessed capillary channel), which are present with stamp Shore A Hardness of 46 (Fig. a), disappear with stamp Shore A Hardness of 57 (Fig. b). Both imprints were made at 10.2 cm/min web speed and 8.9 N of web tension. This web tension was necessary for full feature filling. Colors in (a) and (b) correspond to heights across the structure as shown in the inset scale.

To improve the mechanical performance further, changing the stamp material is another possibility, 37,42 but Sylgard 184 has key advantages for the current work. First, this silicone is readily

available at low cost to facilitate economical stamp fabrication as new circuits and features are under development. Second, this material has a low viscosity when mixed (~ 3.5 Pa•s),<sup>45</sup> which promotes flow of the stamp material into all small features of the master pattern without the need to apply vacuum during casting. Third, silicone-based materials, such as Sylgard 184, have low surface energy (22-23 mJ/cm²)<sup>45</sup>. This low surface energy promotes successful delamination of the cured UV-resin from the imprinting stamp.

# Application of Pressure During Roll-to-Roll Imprinting

1

2

3

4

5

6

7

8

9

10

11

12

13

14

15

16

17

18

19

20

21

22

23

The effect of pressure from web tension and a localized air knife on feature reproducibility is shown in Figure 5. The stamp in this example contains a lattice of narrow raised features that produce a molded pattern of 10  $\mu$ m tall square pillars (40  $\mu$ m x 40  $\mu$ m) separated by 5  $\mu$ m wide recessed capillary channels. (See Figure S7 for the imprinting stamp structure.) This stamp simulates the scenario of closely spaced design elements. The challenge in imprinting this stamp is to uniformly fill all of the square elements. Proper pressure between the coated web and the imprinting stamp forces all air from the pattern features and leads the resin to mold into the shape of the features of the imprinting stamp. Figures 5a and 5c show the reproduction of stamp features with the 8.9 N web tension alone. It should be noted the web tension fluctuates by as much as 10% during imprinting, based on the machine readouts. The tension pulls the web inwards (toward the center of the imprinting drum). The applied pressure measured with a thin film force sensing resistor (Interlink Electronics #34-00068) placed between the web and the imprinting stamp was found to be approximately 2 kPa. In this case, the pillars are incomplete, indicating that that the liquid resin does not flow into all of the recesses in the stamp. A backing roller (55 Shore A Hardness) was tested as a method for applying increased imprinting pressure; however, the smallest amount of applied force from the backing roller (13 N) was observed to significantly

distort the imprints and cause excessive resin extrusion (See Figure S8). Increased buckling of high-aspect ratio features of the stamp was observed with the backing roller. Thus, an air knife was investigated as a method of applying smaller amounts of force during imprinting. Figure 5b and 5d show that the addition of an air knife leads to complete filling, and the intended network of pillars and recessed capillary channels is fully reproduced. The air knife applies pressure to the backside of the PET web at the point of first contact between the coated PET web and the imprinting stamp, assisting with the filling of the UV resin into the recessed areas of the stamp. The pressure applied by the air knife at the point of impingement between the web and the imprinting stamp was measured to be approximately 1.2 kPa in addition to the pressure supplied by web tension. It should be noted that the air knife was not observed to alter the imprinting pressure anywhere else around the imprinting drum. This locally applied pressure mitigates the need for increased web tension throughout the entire imprinting apparatus. This enhanced two-part application of pressure together with the improved PDMS tensile storage and loss moduli led to successful reproduction of high aspect ratio features.

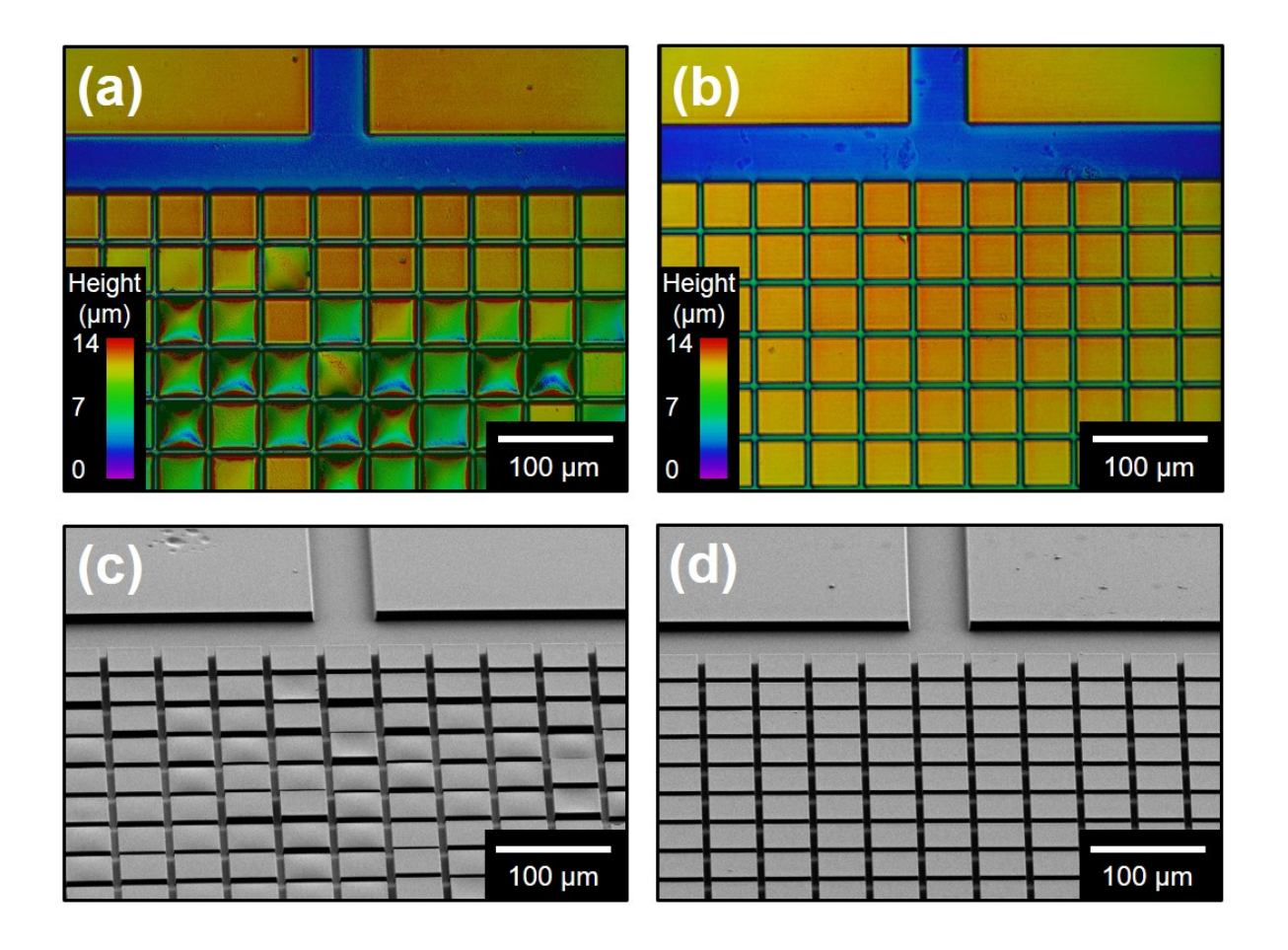


**Figure 5.** Comparison of imprinting performance achieved without and with the air knife applying additional pressure to the web: (a and c) Confocal and SEM images, respectively, of 5  $\mu$ m wide, 10  $\mu$ m deep recessed channels with 40  $\mu$ m x 40  $\mu$ m pillars between them *without* the air knife pressure, showing incomplete reproduction and inconsistent height for most of the pillars; (b and d) confocal and SEM images, respectively of 5  $\mu$ m wide, 10  $\mu$ m deep recessed channels with 40  $\mu$ m x 40  $\mu$ m pillars between them *with* the air knife pressure, showing complete reproduction and consistent pillar height. Colors in (a) and (b) correspond to heights across the structure as shown in the inset scale.

# Roll-to-Roll Imprinting of Capillary Channels for Conductive Lines

Figure 6 shows the first approach used to create deep and narrow capillary channels needed for high current carrying conductors – the recessed design. This approach employs a stamp with tall, narrow features (Fig. 6a) that create recessed capillaries in the UV curable layer (Fig. 6b). Figures 6c and 6d show the stamp and finished imprint, respectively, for a 3  $\mu$ m wide and 20  $\mu$ m

deep channel ( $\varepsilon \sim 7$ ). Overview SEM images of this imprinted structure are shown in the supporting material (Figs. S2a and S2c). The width and depth of the channels imprinted in the UV curable resin are identical (within measurement error) to the width and depth of the channels in the Si master. From the cross-section image of the channel shown in Figure 6e, nearly vertical walls are maintained along the length of the capillary channel (cross sectional image is taken midway between reservoirs). The tapered channel walls result from the etching treatment used to make the master and do not adversely affect the performance of conductors and may facilitate separation of the stamp from the imprinted channel. As shown in the confocal microscope image of the imprinted capillary channel and reservoir in Figure 6f, uniform elevation is achieved across the imprint, both in the indented area (the blue reservoir) and across the area outside the feature (the orange area). The imprinting process accurately reproduces the features on the master pattern across the full surface face of the imprinting stamp. Large and small features are successfully imprinted at the same time. For example, Figure 6f shows a 750  $\mu$ m diameter reservoir and a 3  $\mu$ m wide capillary channel imprinted in close proximity.

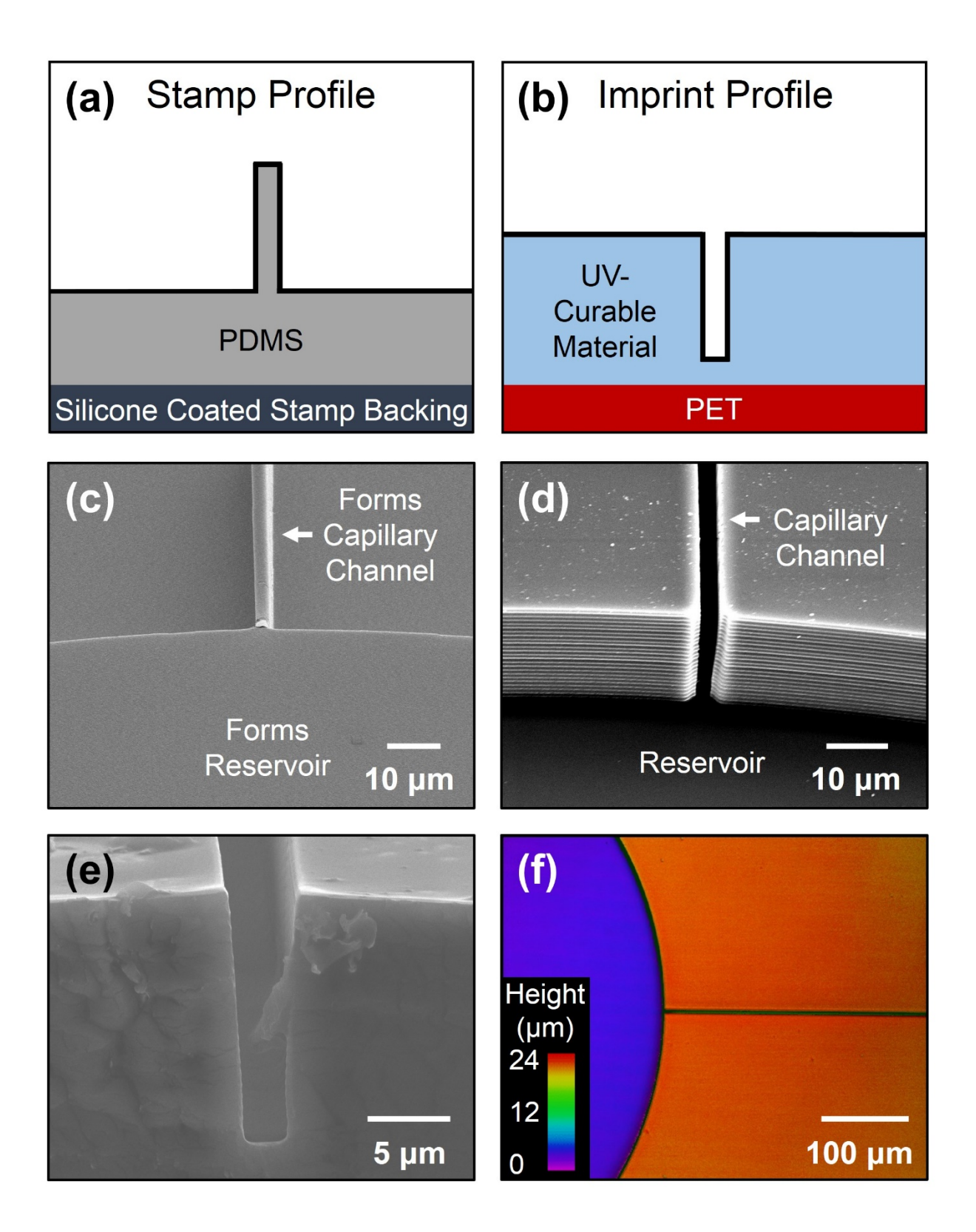


**Figure 6.** (a) & (b) Schematic of the imprinting process for creating capillary channels using the recessed design, (c) SEM image of the imprinting stamp used to form recessed capillary channels, (d) SEM image of imprinted capillary channel and reservoir with 3  $\mu$ m wide, 20  $\mu$ m deep channel,

(e) SEM image of the cross section of the capillary channel, and (f) confocal microscope image of the capillary channel and reservoir showing good uniformity across the substrate surface.

2 3

Forming deeper channels using the recessed design presented in Figure 6 is challenging for several reasons. First, deeper channels require thicker layers of UV-curable resin. For example, to imprint a 50  $\mu$ m deep channel using this method, a coated layer thickness of at least 50  $\mu$ m is required. Depending on the UV-curable resin formulation, thicker layers could suffer from greater attenuation of UV intensity through the thickness and hence require a more powerful UV source or a slower processing speed to cure. A thicker layer of UV-curable resin also increases the cost of the fabricated device and decreases flexibility. Lastly, the high aspect ratio part of the stamp, which forms the conductor, is the highest point on the stamp, making the stamp susceptible to damage. As the aspect ratio increases so does the susceptibility to buckling. An expression for the critical buckling force ( $F_{cs}$ ) for rectangular slab features on the PDMS stamp can be expressed as:

15 
$$F_{Crit} = \frac{\pi E L_f W_f^3}{48 H_f^2}$$
 (2)

where E is Young's modulus,  $L_f$  is feature length,  $W_f$  is feature width, and  $H_f$  is feature height. This expression is representative of portions of the stamp that form recessed capillary channels away from the reservoirs. In this case, the stamp dimensions mirror the recessed capillary dimensions (Fig. 6c), and therefore  $F_{cm}$  is reduced as  $W_f$  narrows and  $H_f$  increases (*i.e.*, as aspect ratio of conductive channels increases).

Using the alternative raised design, walls form deep capillary channels, as shown in Figure 7, which overcomes the challenges noted for recessed channels. To form raised walls, a stamp is fabricated as shown in the schematic of Figure 7a. The stamp contains indents where raised features are desired on the finished imprint, which is shown in Figure 7b. When this stamp is

pressed into the UV resin, the UV resin is displaced from where the low areas of the imprint are formed and flows into the raised areas, filling them. Figure 7c and 7d show SEM images of the stamp and finished imprint, respectively, for  $50~\mu m$  tall,  $30~\mu m$  wide raised walls, which form a capillary channel  $10~\mu m$  wide. Overview images of the structure are shown in the supporting information (Figs. S2b and S2d). The imprinting pressures achievable on our roll-to-roll system from web tension and the air knife molds UV resin into these  $50~\mu m$  tall raised features from the 25  $\mu m$  thick coating of UV-curable resin. It is worth noting that the walls do not occupy a large fraction of the stamp area and hence there is sufficient resin present to form them. These  $50~\mu m$  tall features also fully cure in our system at a web speed of 10.2~cm/min without the need for higher UV powers or slower speed. Additionally, the high aspect ratio piece of the stamp is not the highest point on the stamp, which significantly improves durability and leads to resistance against buckling.

With this method of imprinting, we have been able to form capillary channels as deep as  $50 \, \mu \text{m}$  and as narrow as  $10 \, \mu \text{m}$  (Fig. 7). A consistent width along the length of the channel is shown in the cross-sectional and confocal images (Fig. 7e and 7f, respectively). However, the depth of the channel decreases slightly ( $\sim 10\%$ ) with distance away from the reservoir. This variation is linked to the fabrication of the Si master. Etch rates of the method used to create the Si master are lower in between the raised walls as compared with the wide flat areas outside the channel. The depth variation is significantly less in wider channels, as demonstrated by the cross section of a  $30 \, \mu \text{m}$  wide,  $50 \, \mu \text{m}$  deep channel shown in Figure S9. As shown in Figure 7f, consistent heights are achieved across the main surface of the imprint. The UV imprinted pattern is an accurate reproduction of the initial master silicon pattern.

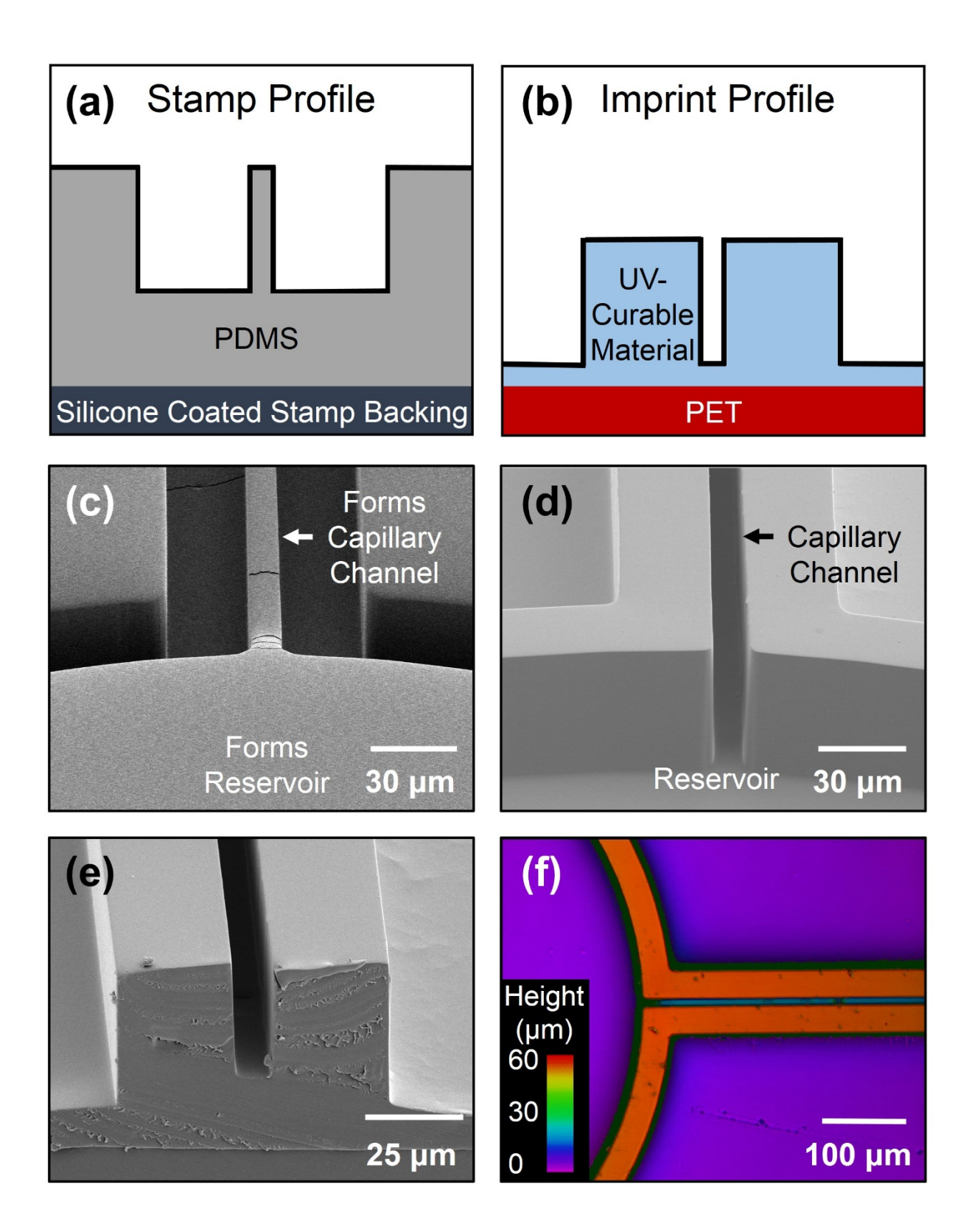


**Figure 7.** (a) & (b) Schematic of the imprinting process for creating capillary channels using the raised wall design, (c) SEM image of the imprinting stamp used to form a capillary channel  $10 \mu m$  wide and  $50 \mu m$  deep between two raised walls, (d) SEM images of imprinted capillary channel

and reservoir with 10  $\mu$ m wide channel, 50  $\mu$ m deep with 30  $\mu$ m wide walls, (e) SEM image of the cross section of the capillary channel formed from raised walls, and (f) confocal microscope image of the capillary channel formed from walls showing good uniformity across the substrate surface.

4 5

6

7

8

9

10

11

12

13

14

15

16

17

18

19

20

21

22

23

24

25

1

3

# Conductors from Imprinted Capillary Channels

Imprinted capillary channels are converted into conductors by filling them with conductive material, as shown in Figure 8. A schematic of the process used is given in the supporting information (Fig. S6). First, drop-on-demand inkjet printing is used to deposit an aqueous silver ink<sup>50</sup> into the reservoirs connected to the channels. Capillarity-driven flow fills the channel from the reservoir. The silver ink wets the channel (contact angle  $\sim 0^{\circ}$ ), which is necessary for flow; the flow distance depends on the ink properties, such as surface tension and viscosity as well as channel geometry and drying conditions.<sup>51</sup> More information on flow and drying in capillaries is given by Lade, et al. Figure S10 in the supporting information shows data for silver ink flow length in recessed capillaries. Flow distances greater than 1 cm are achieved in 20  $\mu$ m deep capillaries with the silver ink used here. Longer conductors may be required for large area circuits, but a key feature of SCALE is device miniaturization. Longer conductors are possible by placing multiple reservoirs along the length of the channel or by altering humidity and drying conditions. Addressing this need is an area of ongoing research. The ink contained in the channel is pinned at the channel's top edge, as explained by Gibbs criterion<sup>22</sup>. The aqueous silver ink deposition and annealing was repeated for each conductor in this study to lower electrical resistance and improve repeatability. After annealing the silver ink, a thin film of silver ( $\sim 1 \, \mu \text{m}$  thick) is left in the channel as shown in Figure 8b and 8e (top down view) and in Figure 8h (cross-section view).

The printed silver layer serves as a seed layer for the second step in the process, selective copper electroless plating. The printed substrates are submerged in an electroless plating solution

for a specified amount of time to allow the copper to grow on the silver. The copper deposits in the channels as shown in Figure 8c, 8f, and 8i. Since the copper only deposits where the silver has been printed, thick, precisely positioned conductors are created. A slight, but noticeable increase ( $\sim 15\%$ ) in channel width is observed after the copper deposition process, which leads to a final conductor width that is slightly larger than the initial capillary width. Research is ongoing to address and understand the origin of this distortion and improve the deposition of metal in the channel. Additionally, strategies to reduce the plating time are being investigated since the electroless plating is currently the slowest step in the conductor fabrication process. The origin of this width increase is a topic of current investigation. Using this process, we have formed printed conductors as narrow as 3  $\mu$ m on the roll-to-roll imprinted substrates, as shown in the supporting information (Fig. S11). This resolution and high aspect ratio are significantly higher than those for printing techniques such as gravure and direct inkjet printing.

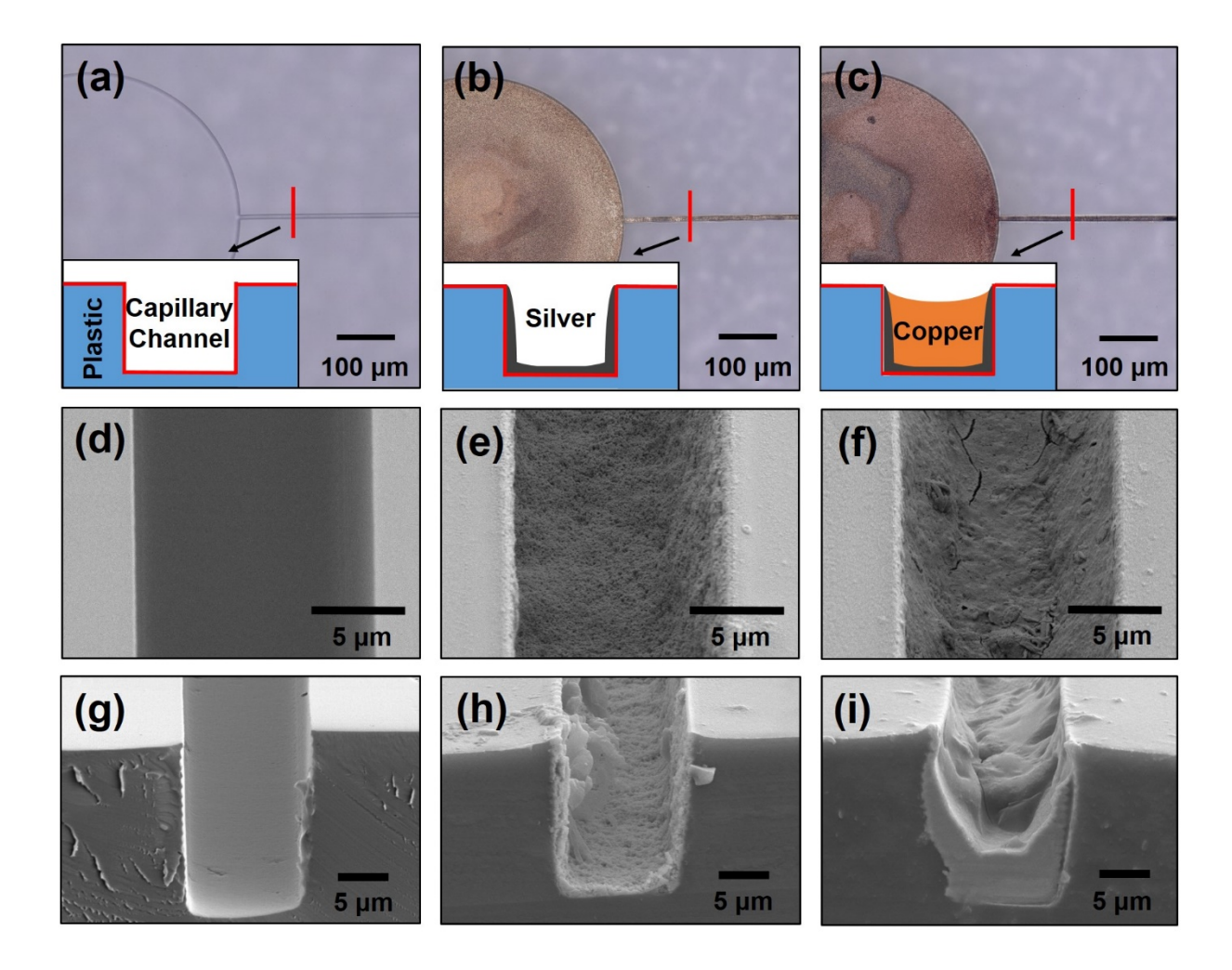


**Figure 8.** Microscope images and schematics of the fabrication process for creating a SCALE conductor in a recessed channel consisting of (a) imprinting the plastic substrate, (b) printing a silver ink seed layer into the capillary channels, and (c) copper electroless plating to create conductors. Top view SEM images of capillary channels at each step of the process (d) empty, (e) after silver printing, and (f) after copper electroless plating. Cross sectional SEM images of each step in the process (g) empty, (h) after silver printing, and (i) after copper electroless plating.

To characterize the resistance of printed conductors, capillaries of various lengths with a reservoir at each end were imprinted using the recessed design. The reservoirs feed ink into the channel and serve as contact points for probes in the two-point probe resistance measurement. Conductors were created using inkjet printing of silver ink into the reservoirs and copper electroless plating, as described above.

Resistance as a function of capillary length for the channels prepared using the recessed design and only containing annealed silver ink is shown in Figure 9a. Resistance increases with length and decreases with width of channel, as expected from Eq. 1. However, resistance does not increase linearly with length. The nonlinearity suggests that the silver layer does not have consistent cross-sectional area as channel length increases, assuming that the resistivity is not affected by channel length. At longer lengths the silver cross-sectional area apparently drops, which indicates a thinner silver layer is deposited.

Figure 9b shows that the resistance markedly decreases when the silver printing is followed with copper plating. Internal measurement system resistance has been subtracted from this plot by applying a linear fit. Raw data without the correction are plotted in Figure S12. The plating significantly increases the metal content in the channel, which corresponds to the significant decrease in resistance. Resistance increases linearly with conductor length, as expected for a constant cross-sectional area and resistivity. This fabrication strategy of first printing silver ink and then depositing copper to fill the channel has been used to successfully fabricate conductors in  $10 \,\mu\text{m}$  wide capillary channels with linear resistance as low as  $0.46 \,\Omega/\text{mm}$  and conductors in  $20 \,\mu\text{m}$  wide capillary channels with linear resistance as low as  $0.24 \,\Omega/\text{mm}$ . All channels were  $20 \,\mu\text{m}$  deep recessed capillaries. Hence, the conductor resistance scales linearly with channel width as expected.

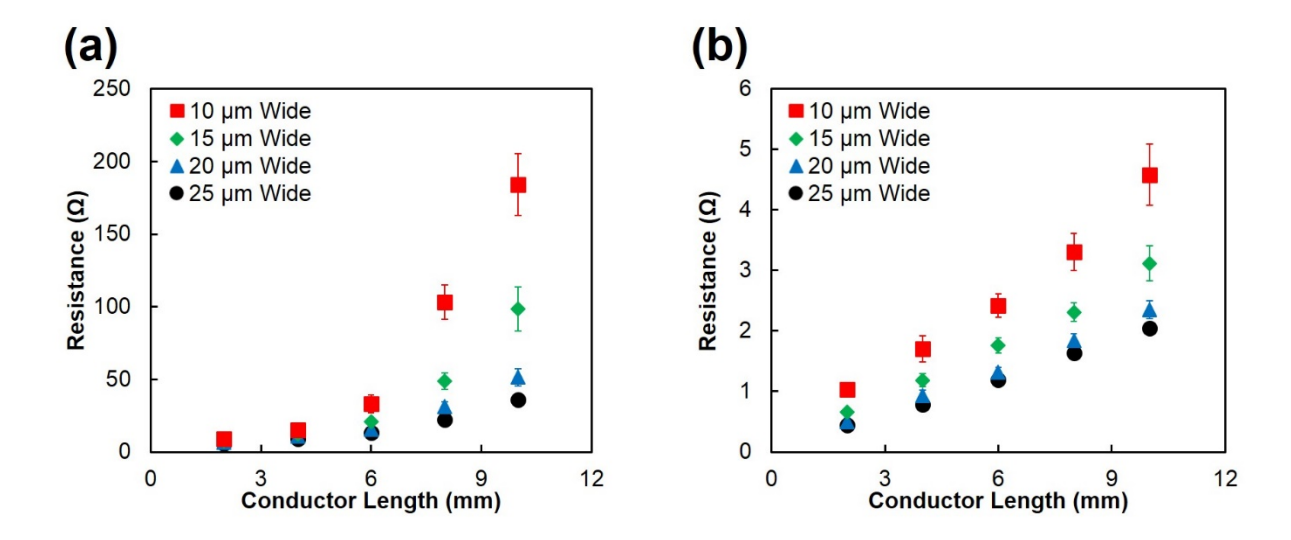


**Figure 9.** Resistance of capillary conductors fabricated from roll-to-roll imprinted recessed channel substrates: (a) with two depositions of 30 drops of silver ink in the reservoir at each end of the channel and (b) after copper electroless plating on top of the printed silver for 60 minutes with contact resistance subtracted. Note, all channels are  $20 \, \mu \text{m}$  deep.

Using deeper channels (50  $\mu$ m) formed with raised walls, it is possible to fabricate conductors with larger cross-sections, and consequently significantly lower resistances per length (R/L), without increasing the required substrate surface area. The channel geometry shown in Figure 7 was used to form conductors by the fabrication scheme shown in Figure S6. These conductors demonstrate linear resistance as low as  $0.034~\Omega/mm$  for a printed conductor in a  $30~\mu m$  capillary (aspect ratio of  $\sim 1.6$ ). Note that an increase in channel width is again observed during the copper plating process, but this is not detrimental to conductor performance. Optical microscopy top views of these conductors and SEM images looking down the length of the conductor from the reservoir are shown in the supporting information (Fig. S13). These images demonstrate that solid conductors with consistent cross sections can be formed even in these deep channels with aspect ratios of  $\sim 5$ . The tall conductors also have significantly lower resistance than the shallower capillary channel conductors as expected. Resistance data for these conductors as a

- 1 function of channel geometry is given in the supporting information (Fig. S14). Similar to the
- 2 shallower conductors, these data show a clear linear dependence of resistance on conductor length
- 3 and a decrease in resistance as the conductors become wider as expected.

# Forming Conductors into Networks

Figure 10 shows examples of interconnected conductor networks in which multiple locations are connected with a single printing operation. The ability to make this connection with ink deposition in a single location is a distinct advantage of the SCALE process as compared to traditional printing methods. Figures 10a and 10b show seven-point and nine-point interconnects, respectively. These structures consist of multiple imprinted reservoirs (intended to represent locations in a circuit to electrically connect) joined together with a network of recessed capillary channels. Inkjet printing was used to deposit ink only in the reservoirs marked with an asterisk (\*). Then, capillary force drives the ink along the channels, and the flow branches at each junction so that it reached each of the other reservoirs. As shown in Figure 10b, this approach has successfully connected together nine reservoirs from inkjet printing into only a single location.

Measured resistances for each conductor (the path between every possible pair of reservoirs) are shown in Figure 10c for the nine-point interconnect as a function of the conductor length. The data show a linear dependence of resistance on conductor length as expected. To characterize the consistency, Figure 10d shows the resistance per length (R/L) plotted against the average distance of the conductor from the printed reservoir marked with the asterisk. The conductors have a consistent R/L independent of the distance from the printed reservoir, which is consistent with uniform ink distribution throughout the printed device. Other interconnect geometries are shown in supplemental Figure S15, including an example of a seven-point

- 1 interconnect where ink has been deposited into each of the reservoirs. These results demonstrate
- 2 we can reliably connect multiple locations with ink deposition into a single location.

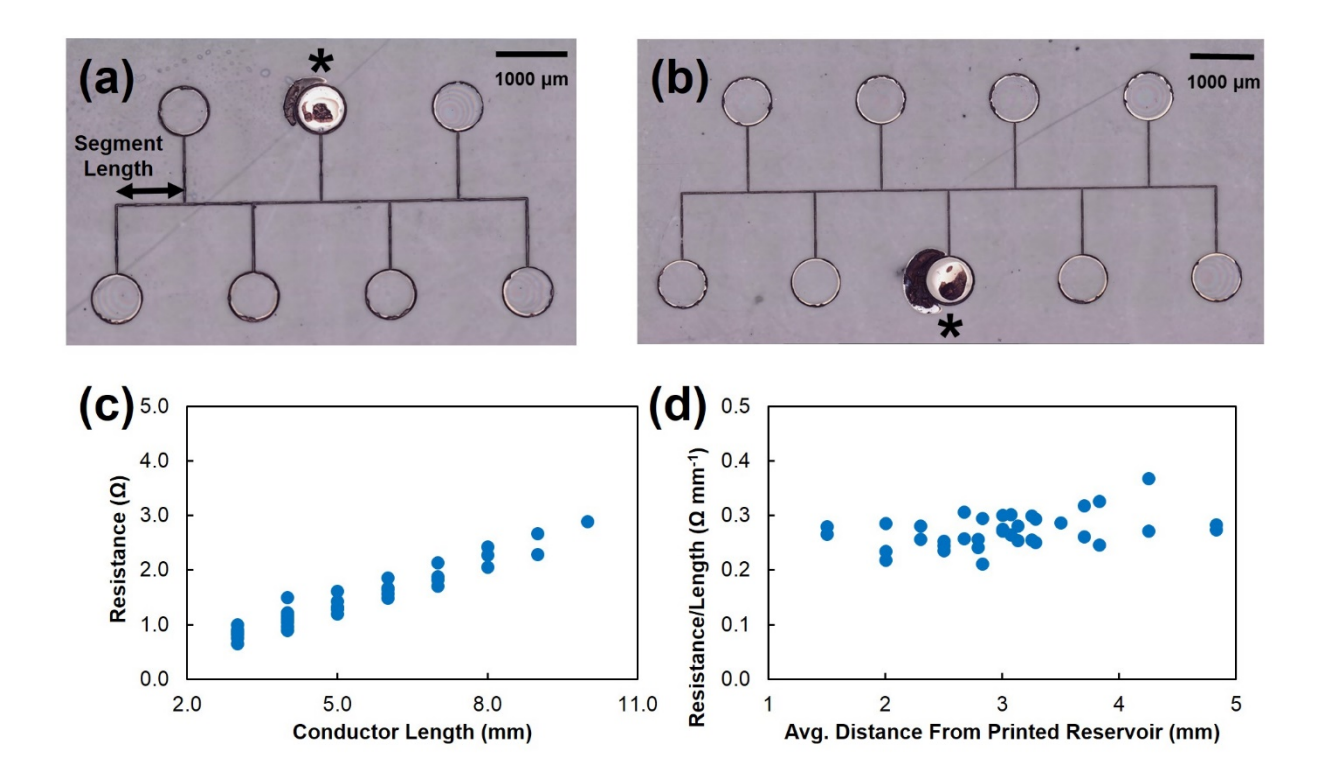


**Figure 10.** (a) Multipoint capillary interconnect with seven locations connected from one printed reservoir (marked with \*), (b) multipoint capillary interconnect with nine locations connected from one printed reservoir (marked with \*), (c) resistance vs. length of conductor segments taken from the nine-point interconnect with 1.0 mm segment lengths, showing linear resistance dependence on length, and (d) resistance/length of conductor segments vs. distance between the printed reservoir and segment taken from the nine-point interconnect, showing a constant R/L.

Other complex conductor geometries in addition to branched conductors, such as curved and bent conductors, are also possible. Figure 11 shows examples of bent conductors formed with the fabrication strategies outlined in this work. This demonstrates that our fabrication process is not limited to straight line conductors.

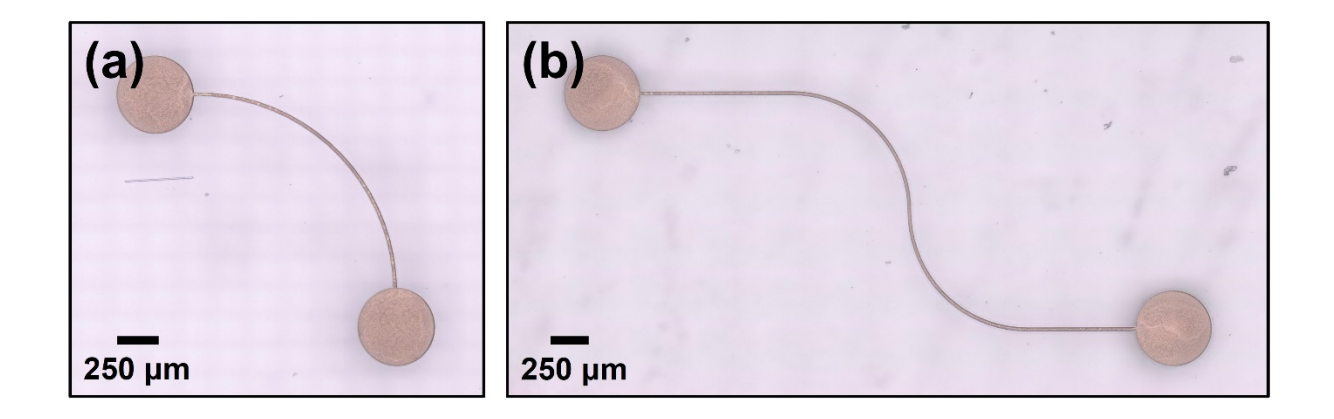


**Figure 11.** Capillary conductors formed by printing on substrates prepared by roll-to-roll imprinting as described in this work, demonstrating bent and curved conductors (a) 90 ° curved conductor and (b) s-bend conductor. All channels are 20  $\mu$ m deep and 10  $\mu$ m wide and printed with aqueous silver ink.

#### **Conclusions:**

In this work, we have demonstrated an efficient method for fabricating roll-to-roll imprinting stamps, which are capable of reproducing micron scale, high aspect ratio raised and recessed features in a UV curable coating on a flexible plastic substrate. These stamps allow for easy fabrication of different feature geometries for testing purposes and possible production of future electronic devices. The fabrication process of these stamps utilizes low-cost liquid casting to reproduce a reusable master pattern. The stamps were installed in our roll-to-roll imprinting system to enable the fabrication of molded structures required for forming high resolution, high aspect ratio conductors that are the basic building blocks of electrical circuits. These conductors have very low resistance per length values (as low as  $0.034~\Omega/mm$ ) and high uniformity. Low resistance conductors could be of special use to transmit power from printed batteries or printed photovoltaic cells, for example. Conductive networks were fabricated with multipoint interconnects that electrically join multiple (up to nine is shown in this work) locations in a circuit after ink deposition into a single location. The techniques developed in this work serve as the

- building blocks for adapting all SCALE device structures, including transistors and other electrical
- 2 components, to roll-to-roll processing. Continued research is focussed on increasing overall
- 3 imprinting speed and improving the quality and speed of the copper plating process.

5

### ASSOCIATED CONTENT

- 6 The following information is available free of charge:
- 7 Schematic illustration of the master wafer fabrication process; overview SEM images of the
- 8 recessed and raised capillary geometries; optical and confocal images of cells on the gravure roller;
- 9 close up annotated photographs of the reverse gravure coating and imprinting processes used in
- this work; schematic illustration of the conductor fabrication process; SEM image of the imprinting
- stamp used to form imprinted grid structures; confocal microscope image of a channel imprinted
- with a backing roller; cross sectional SEM image of a raised wall capillary 30  $\mu$ m wide; measured
- capillary flow distance data for the aqueous silver ink used in this work; optical and SEM images
- of a 3  $\mu$ m wide conductor fabricated using the SCALE process; raw data of resistance vs. conductor
- length for copper plated, recessed channels; optical and SEM images for deep capillary channel
- 16 conductors formed from raised walls; measured resistance values for deep conductors; and optical
- images of other interconnect geometries. (PDF)

18

19

### **AUTHOR INFORMATION**

- 20 Corresponding Authors
- \*E-mail: frisbie@umn.edu. (C.D.F.), \*E-mail: lfrancis@umn.edu. (L.F.F.)
- 22 Author Contributions
- 23 The manuscript was written through contributions of all authors. All authors have given approval

- 1 to the final version of the manuscript.
- 2 Notes
- 3 The authors declare no competing financial interests.

# 5 ACKNOWLEDGMENTS

6 This work was initially supported by the Multi-University Research Initiative (MURI) program 7 sponsored by the Office of Naval Research (MURI Award No. N00014-11-1-0690) and then by 8 the National Science Foundation (NSF Award No. CMMI-1634263). K. S. J. gratefully 9 acknowledges support from the NSF Graduate Research Fellowship Program under Grant No. 10 (00039202). Any opinions, findings, and conclusions or recommendations expressed in this 11 material are those of the authors and do not necessarily reflect the views of the National Science 12 Foundation. The authors thank F. Zare Bidoky, Dr. D. Song, and Dr. W. J. Hyun for valuable 13 discussion. The authors thank S. B. Walker and J. L. Lewis for the silver ink used in this research. 14 Parts of this work were carried out in the Characterization Facility, University of Minnesota, which 15 receives partial support from NSF through the MRSEC program. Portions of this work were 16 conducted in the Minnesota Nano Center, which is supported by the National Science Foundation 17 through the National Nano Coordinated Infrastructure Network (NNCI) under Award Number 18 ECCS-1542202...

### 1 REFERENCES

- 2 (1) Rida, A.; Yang, L.; Vyas, R.; Bhattaeharya, S.; Tentzeris, M. M. Design and Integration of
- 3 Inkjet-Printed Paper-Based UHF Components for RFID and Ubiquitous Sensing Applications.
- 4 *Proc. 37th Eur. Microw. Conf. EUMC* **2007**, 724–727.
- 5 (2) Subramanian, V.; Fréchet, J. M. J.; Chang, P. C.; Huang, D. C.; Lee, J. B.; Molesa, S. E.;
- 6 Murphy, A. R.; Redinger, D. R.; Volkman, S. K. Progress Toward Development of All-Printed
- 7 RFID Tags: Materials, Processes, and Devices. *Proc. IEEE* **2005**, *93* (7), 1330–1338.
- 8 (3) Andersson, P.; Nilsson, D.; Svensson, P. O.; Chen, M.; Malmström, A.; Remonen, T.;
- 9 Kugler, T.; Berggren, M. Active Matrix Displays Based on All-Organic Electrochemical Smart
- 10 Pixels Printed on Paper. Adv. Mater. **2002**, 14 (20), 1460–1464.
- 11 (4) Berggren, M.; Nilsson, D.; Robinson, N. D. Organic Materials for Printed Electronics. *Nat*.
- 12 *Mater.* **2007**, *6* (1), 3–5.
- 13 (5) Hoth, C. N.; Schilinsky, P.; Choulis, S. A.; Brabec, C. J. Printing Highly Efficient Organic
- 14 Solar Cells. *Nano Lett.* **2008**, 8 (9), 2806–2813.
- 15 (6) Hübler, A.; Trnovec, B.; Zillger, T.; Ali, M.; Wetzold, N.; Mingebach, M.; Wagenpfahl,
- 16 A.; Deibel, C.; Dyakonov, V. Printed Paper Photovoltaic Cells. Adv. Energy Mater. 2011, 1 (6),
- 17 1018–1022.
- 18 (7) Khan, Y.; Ostfeld, A. E.; Lochner, C. M.; Pierre, A.; Arias, A. C. Monitoring of Vital Signs
- 19 with Flexible and Wearable Medical Devices. *Adv. Mater.* **2016**, 28 (22), 4373–4395.
- 20 (8) Chang, W. Y.; Fang, T. H.; Sheh, Y. T.; Lin, Y. C. Flexible Electronics Sensors for Tactile
- 21 Multiscanning. Rev. Sci. Instrum **2009**, 80, 084701–084716.

- 1 (9) Meier, B.; Egermann, L.; Voigt, S.; Stanel, M.; Kempa, H.; Huebler, A. C. Drift in the
- 2 Resistance of Poly(3,4-Ethylenedioxythiophene):Poly(Styrenesulfonate) Printed Films during
- 3 Thermal Cycling. *Thin Solid Films* **2011**, *519* (19), 6610–6612.
- 4 (10) Knobloch, A.; Manuelli, A.; Bernds, A.; Clemens, W. Fully Printed Integrated Circuits
- 5 from Solution Processable Polymers. *J. Appl. Phys.* **2004**, *96* (4), 2286–2291.
- 6 (11) Drury, C. J.; Mutsaers, C. M. J.; Hart, C. M.; Matters, M.; de Leeuw, D. M. Low-Cost All-
- 7 Polymer Integrated Circuits. *Appl. Phys. Lett.* **1998**, *73* (1), 108–110.
- 8 (12) Szczech, J. B.; Megaridis, C. M.; Zhang, J.; Gamota, D. R. Ink Jet Processing of Metallic
- 9 Nanoparticle Suspensions for Electronic Circuitry Fabrication. *Microscale Thermophys. Eng.*
- 10 **2004**, 8 (4), 327–339.
- 11 (13) Perelaer, J.; Smith, P. J.; Mager, D.; Soltman, D.; Volkman, S. K.; Subramanian, V.;
- 12 Korvink, J. G.; Schubert, U. S. Printed Electronics: The Challenges Involved in Printing Devices,
- 13 Interconnects, and Contacts Based on Inorganic Materials. J. Mater. Chem. 2010, 20 (39), 8446.
- 14 (14) Lilja, K. E.; Bäcklund, T. G.; Lupo, D.; Hassinen, T.; Joutsenoja, T. Gravure Printed
- Organic Rectifying Diodes Operating at High Frequencies. Org. Electron. physics, Mater. Appl.
- 16 **2009**, *10* (5), 1011–1014.
- 17 (15) Mahajan, A.; Frisbie, C. D.; Francis, L. F. Optimization of Aerosol Jet Printing for High
- 18 Resolution, High Aspect Ratio Silver Lines. ACS Appl. Mater. Interfaces 2013, 5 (11), 4856–4864.
- 19 (16) Lee, H. H.; Chou, K. Sen; Huang, K. C. Inkjet Printing of Nanosized Silver Colloids.
- 20 Nanotechnology **2005**, 16 (10), 2436–2441.

- 1 (17) Khan, S.; Lorenzelli, L.; Dahiya, R. S. Technologies for Printing Sensors and Electronics
- 2 over Large Flexible Substrates: A Review. *IEEE Sens. J.* **2015**, *15* (6), 3164–3185.
- 3 (18) Homenick, C. M.; James, R.; Lopinski, G. P.; Dunford, J.; Sun, J.; Park, H.; Jung, Y.; Cho,
- 4 G.; Malenfant, P. R. L. Fully Printed and Encapsulated SWCNT-Based Thin Film Transistors via
- 5 a Combination of R2R Gravure and Inkjet Printing. ACS Appl. Mater. Interfaces 2016, 8 (41),
- 6 27900–27910.
- 7 (19) Applications of Organic and Printed Electronics: A Technology-Enabled Revolution;
- 8 Cantatore, E., Chandrakasan, A. P., Eds.; Springer: Boston, 2013.
- 9 (20) Nguyen, H. A. D.; Lee, C.; Shin, K. H. A Mathematical Model to Predict Surface
- 10 Roughness and Pattern Thickness in Roll-to-Roll Gravure Printed Electronics. Robot. Comput.
- 11 *Integr. Manuf.* **2013**, 29 (4), 26–32.
- 12 (21) Kim, K. S.; Jung, K. H.; Jung, S. B. Design and Fabrication of Screen-Printed Silver
- 13 Circuits for Stretchable Electronics. *Microelectron*. Eng. **2014**, 120, 216–220.
- 14 (22) Zhang, X.; Liu, K.; Sunappan, V.; Shan, X. Diamond Micro Engraving of Gravure Roller
- Mould for Roll-to-Roll Printing of Fine Line Electronics. J. Mater. Process. Technol. 2015, 225,
- 16 337–346.
- 17 (23) Hyun, W. J.; Zare Bidoky, F.; Walker, S. B.; Lewis, J. A.; Francis, L. F.; Frisbie, C. D.
- Printed, Self-Aligned Side-Gate Organic Transistors with a Sub-5 Um Gate-Channel Distance on
- 19 Imprinted Plastic Substrates. *Adv. Electron. Mater.* **2016**, 2, 1600293–1600300.

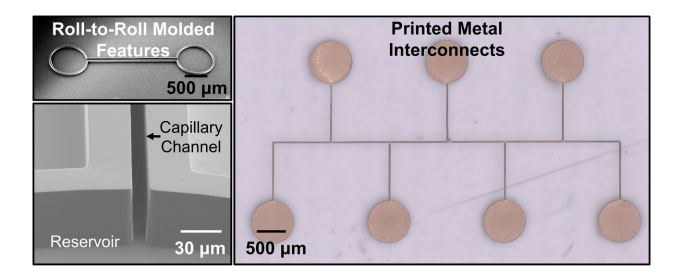
- 1 (24) Zare Bidoky, F.; Frisbie, C. D. Parasitic Capacitance Effect on Dynamic Performance of
- 2 Aerosol-Jet-Printed Sub 2 V Poly(3-Hexylthiophene) Electrolyte-Gated Transistors. ACS Appl.
- 3 *Mater. Interfaces* **2016**, 8 (40), 27012–27017.
- 4 (25) Kang, H.; Kitsomboonloha, R.; Jang, J.; Subramanian, V. High-Performance Printed
- 5 Transistors Realized Using Femtoliter Gravure-Printed Sub-10 Um Metallic Nanoparticle Patterns
- and Highly Uniform Polymer Dielectric and Semiconductor Layers. Adv. Mater. 2012, 24 (22),
- 7 3065–3069.
- 8 (26) Le Bourvellec, G.; Beautemps, J. Stretching of PET Films under Constant Load. II.
- 9 Structural Analysis. J. Appl. Polym. Sci. **1990**, 39 (2), 319–328.
- 10 (27) Song, D.; Zare Bidoky, F.; Hyun, W. J.; Walker, S. B.; Lewis, J. A.; Frisbie, C. D. All-
- 11 Printed, Self-Aligned Carbon Nanotube Thin-Film Transistors on Imprinted Plastic Substrates.
- 12 ACS Appl. Mater. Interfaces **2018**, 10 (18), 15926–15932.
- 13 (28) Mahajan, A.; Hyun, W. J.; Walker, S. B.; Lewis, J. A.; Francis, L. F.; Frisbie, C. D. High-
- Resolution, High-Aspect Ratio Conductive Wires Embedded in Plastic Substrates. ACS Appl.
- 15 *Mater. Interfaces* **2015**, 7 (3), 1841–1847.
- 16 (29) Mahajan, A.; Hyun, W. J.; Walker, S. B.; Rojas, G. A.; Choi, J. H.; Lewis, J. A.; Francis,
- 17 L. F.; Frisbie, C. D. A Self-Aligned Strategy for Printed Electronics: Exploiting Capillary Flow on
- 18 Microstructured Plastic Surfaces. Adv. Electron. Mater. 2015, 1 (9), 1500137–1500146.
- 19 (30) Hyun, W. J.; Secor, E. B.; Kim, C. H.; Hersam, M. C.; Francis, L. F.; Frisbie, C. D.
- 20 Scalable, Self-Aligned Printing of Flexible Graphene Micro-Supercapacitors. Adv. Energy Mater.
- 21 **2017**, 7 (17), 1–8.

- 1 (31) Noh, J.; Yeom, D.; Lim, C.; Cha, H.; Han, J.; Kim, J.; Park, Y.; Subramanian, V.; Cho, G.
- 2 Scalability of Roll-to-Roll Gravure-Printed Electrodes on Plastic Foils. *IEEE Trans. Electron*.
- 3 *Packag. Manuf.* **2010**, *33* (4), 275–283.
- 4 (32) Lade, R. K.; Jochem, K. S.; Macosko, C. W.; Francis, L. F. Capillary Coatings: Flow and
- 5 Drying Dynamics in Open Microchannels. *Langmuir* **2018**, *34* (26), 7624–7639.
- 6 (33) Yang, D.; Krasowska, M.; Priest, C.; Ralston, J. Dynamics of Capillary-Driven Flow in
- 7 Open Microchannels. J. Phys. Chem. C 2011, 115, 18761–18769.
- 8 (34) Ahn, S. H.; Guo, L. J. High-Speed Roll-to-Roll Nanoimprint Lithography on Flexible
- 9 Plastic Substrates. Adv. Mater. 2008, 20 (11), 2044–2049.
- 10 (35) Ahn, S.; Cha, J.; Myung, H.; Kim, S. M.; Kang, S. Continuous Ultraviolet Roll
- Nanoimprinting Process for Replicating Large-Scale Nano- and Micropatterns. *Appl. Phys. Lett.*
- 12 **2006**, 89 (21), 1–4.
- 13 (36) Sabik, S.; de Riet, J.; Yakimets, I.; Smits, E. High Resolution Patterning for Flexible
- 14 Electronics via Roll-to-Roll Nanoimprint Lithography. Proc. SPIE Int. Soc. Opt. Eng. 2014,
- 15 *9049*, 90490F.
- 16 (37) Kooy, N.; Mohamed, K.; Pin, L. T.; Guan, O. S. A Review of Roll-to-Roll Nanoimprint
- 17 Lithography | Nanoscale Research Letters | Full Text. *Nanoscale Res. Lett.* **2014**, 9 (1), 1.
- 18 (38) Dumond, J. J.; Mahabadi, K. A.; Yee, Y. S.; Tan, C.; Fuh, J. Y. H.; Lee, H. P.; Low, H. Y.
- 19 High Resolution UV Roll-to-Roll Nanoimprinting of Resin Moulds and Subsequent Replication
- via Thermal Nanoimprint Lithography. *Nanotechnology* **2012**, *23* (48), 485310.

- 1 (39) Han, J.; Choi, S.; Lim, J.; Lee, B. S.; Kang, S. Fabrication of Transparent Conductive
- 2 Tracks and Patterns on Flexible Substrate Using a Continuous UV Roll Imprint Lithography. J.
- 3 Phys. D. Appl. Phys. 2009, 42 (11), 115503.
- 4 (40) Aikio, S.; Hiltunen, J.; Hiitola-Keinänen, J.; Hiltunen, M.; Kontturi, V.; Siitonen, S.;
- 5 Puustinen, J.; Karioja, P. Disposable Photonic Integrated Circuits for Evanescent Wave Sensors
- 6 by Ultra-High Volume Roll-to-Roll Method. Opt. Express 2016, 24 (3), 2527.
- 7 (41) Ok, J. G.; Seok Youn, H.; Kyu Kwak, M.; Lee, K. T.; Jae Shin, Y.; Jay Guo, L.; Greenwald,
- 8 A.; Liu, Y. Continuous and Scalable Fabrication of Flexible Metamaterial Films via Roll-to-Roll
- 9 Nanoimprint Process for Broadband Plasmonic Infrared Filters. *Appl. Phys. Lett.* **2012**, *101* (22).
- 10 (42) Kim, H.; Han, J.; Kim, J.; Kim, T.; Kang, S. Fabrication of Metallic Roll Stamp with Low
- 11 Internal Stress and High Hardness by Pulse Reverse Current Electroforming Process. J.
- 12 *Micromechanics Microengineering* **2014**, 24, 125004–125011.
- 13 (43) Yi, P.; Wu, H.; Zhang, C.; Peng, L.; Lai, X. Roll-to-Roll UV Imprinting Lithography for
- 14 Micro/Nanostructures. J. Vac. Sci. Technol. B, Nanotechnol. Microelectron. Mater. Process.
- 15 *Meas. Phenom.* **2015**, *33* (6), 060801.
- 16 (44) Norland Products. Norland Optical Adhesive 73 Product Data Sheet. 2017, pp 1–3.
- 17 (45) Dow Corning. Electronics Sylgard ® 184 Silicone Elastomer Product Information. 2014,
- 18 pp 1–4.
- 19 (46) Cambridge University Engineering Department. *Materials Data Book*; 2003.
- 20 (47) Johnston, I. D.; McCluskey, D. K.; Tan, C. K. L.; Tracey, M. C. Mechanical
- 21 Characterization of Bulk Sylgard 184 for Microfluidics and Microengineering. J.

- 1 *Micromechanics Microengineering* **2014**, *24* (3), 035017.
- 2 (48) Owen, M. J. Why Silicones Behave Funny. Dow Corning 2005, pp 1–11.
- 3 (49) Ashby, M. F. *Materials Selection in Mechanical Design*, 2nd ed.; Butterworth-Heinemann:
- 4 Boston, 1999.

- 5 (50) Walker, S. B.; Lewis, J. A. Reactive Silver Inks for Patterning High-Conductivity Features
- 6 at Mild Temperatures. J. Am. Chem. Soc. 2012, 134 (3), 1419–1421.
- 7 (51) Ouali, F. F.; McHale, G.; Javed, H.; Trabi, C.; Shirtcliffe, N. J.; Newton, M. I. Wetting
- 8 Considerations in Capillary Rise and Imbibition in Closed Square Tubes and Open
- 9 Rectangular Cross-Section Channels. *Microfluid. Nanofluidics* **2013**, *15* (3), 309–326.
- 10 (52) Oliver, J. F.; Huh, C.; Mason, S. G. Resistance to Spreading of Liquids by Sharp Edges. J.
- 11 *Colloid Interface Sci.* **1977**, *59* (3), 568–581.



- 2 Table of Contents Figure for High Resolution, High Aspect Ratio Printed and Plated Metal
- 3 Conductors Utilizing Roll-to-Roll Micro-Scale UV Imprinting with Prototype Imprinting Stamps.